Chinese Journal of Polymer Science Vol. 31, No. 6, (2013), 870–878

Chinese Journal of Polymer Science
© Chinese Chemical Society
Institute of Chemistry, CAS
Springer-Verlag Berlin Heidelberg 2013

INTERDIFFUSION KINETICS OF MISCIBLE POLYMER/POLYMER LAMINATES INVESTIGATED BY ATOMIC FORCE MICROSCOPY*

Yong-gui Liao[a, b], Meng-jun Peng[a], Feng-zhen Liu[a] and Xiao-lin Xie[a, b**]

[a] *Key Laboratory for Large-Format Battery Materials and System, Ministry of Education, School of Chemistry and Chemical Engineering, Huazhong University of Science and Technology, Wuhan 430074, China*

[b] *Wuhan National High Magnetic Field Center, Huazhong University of Science and Technology, Wuhan 430074, China*

Abstract The miscibility of poly(vinyl chloride)/poly(*n*-butyl methacrylate) (PVC/P*n*BMA) blend and the interdiffusion kinetics of PVC/P*n*BMA laminates have been investigated by differential scanning calorimetry (DSC) and atomic force microscopy (AFM), respectively. This blend exhibited a lower critical solution temperature behavior. Below 120 °C, DSC results showed each blend with different PVC contents exhibited only a single glass transition temperature which increased with PVC content, indicating that PVC and P*n*BMA were miscible. After PVC/P*n*BMA laminates were annealed at different temperature for different time, a smooth cross-section across interface was prepared by ultramicrotoming. Combined with topography and phase images of tapping mode AFM, the relative concentration profile, interface width and the relationship between interface width and annealing time could be obtained. In a regime of rubbery/rubbery interdiffusion, the diffusion obeyed a typical Fickian Case-I behavior where the interface width was proportional to the square root of annealing time. The mutual diffusion coefficient was in good agreement with that obtained from DSC and positron annihilation lifetime spectroscopy. However, in the regime of glassy/rubbery interdiffusion, the diffusion followed a typical Case-II behavior where the interface width was proportional to annealing time. These results imply that AFM is a reliable and powerful tool for the investigation of polymer/polymer interdiffusion at a level of polymer chain size.

Keywords: Miscibility; Polymer interface; Interdiffusion; Kinetics; Atomic force microscopy.

INTRODUCTION

The properties of multi-phase multi-component systems in biology[1–3] and materials[4–9], *etc*., always depend on their interfacial microstructures. Diffusion plays a key role in the formation of interface. Compared with the diffusion of small molecules, polymer/polymer interdiffusion is too complex to describe through Fickian diffusion model. Therefore, theories and experimental methods for this interdiffusion are particularly necessary. Since the reptation model was advanced by Doi-Edwards[10] and de Gennes[11], many models, including slow mode[12], fast mode[13] and fast-slow hybrid mode[14] have been proposed. Comparing with the diffusion velocity of molecular chains (v_d) and relaxation velocity of chain segments (v_r), the interdiffusion of polymers can be classified into Case-I behavior for $v_d > v_r$ and Case-II one for $v_d < v_r$, respectively[15]. The interface width is proportional to the time in Case-II and the square root of time in Case-I.

As the development of theories, many kinds of experimental methods have been successfully used for

* This work was financially supported by the Major International (Regional) Joint Research Project of the National Natural Science Foundation of China (No. 51210004), the National Natural Science Foundation of China (No. 50903035), and Chinese Ministry of Education (NCET-11-0174).

** Corresponding author: Xiao-lin Xie (解孝林), E-mail: xlxie@mail.hust.edu.cn

Invited paper dedicated to Professor Fosong Wang on the occasion of his 80th birthday

Received December 4, 2012; Revised January 1, 2013; Accepted January 9, 2013

doi: 10.1007/s10118-013-1268-x

polymer/polymer interffusion behavior such as Rutherford back scattering spectroscopy (RBS)[16], forward recoil spectroscopy (FRES)[17], neutron reflectometry (NR)[18, 19], nuclear reaction analysis (NRA)[20, 21], X-ray reflectivity (XR)[22], positron annihilation lifetime spectroscopy (PALS)[23], nuclear magnetic resonance (NMR)[24], infrared spectroscopy (IR)[25], Raman spectroscopy (RS)[26], secondary ionisation mass spectrometry (SIMS)[22, 27, 28], transmission electron microscopy (TEM)[29], scanning transmission electron microscopy (STEM)[30] and atomic force microscopy (AFM)[31–33]. At atomic scale, only RBS[16], FRES[17], NR[18, 19] and NRA[20, 21] have been used to study the interdiffussion in reciprocal space. If the motion of polymer chains can be observed directly in real space, one can confirm the information from reciprocal space and directly verify the theory of diffusion. Therefore, it is necessary to study the polymer/polymer interdiffusion thermodynamics and kinetics at a level of polymer chain in real space.

In order to avoid the heavy metal staining in TEM[29] and STEM[30], we have successfully studied the interdiffusion kinetics of poly(methyl methacrylate)/poly(styrene-*ran*-acrylonitrile) (PMMA/SAN) by an expensive instrument, energy-filtering TEM, at a resolution of 10 nm[34]. AFM, one of the most important scanning probe microscopies, has become an increasingly popular tool for characterizing the surfaces and interfaces of materials. In a series of previous work, using *in situ* AFM, we have investigated the phase and dewetting behaviors for PMMA/SAN blend films[35–41]. From AFM phase images of the interface of glass fiber reinforced polypropylene and epoxy resin composites polished by silica/alumina, the relative concentration profile across the interface and its width can be obtained[31]. An interface of coextruded multilayer polyolefin films with a width less than 100 nm has also been measured by AFM[32]. Tapping and contact-resonance modes have been used to study the interface of butadiene rubber and styrene-butadiene rubber with a width of 180 nm for miscible system and 30 nm for immiscible one[33]. To our best knowledge, although these studies on the interdiffusion thermodynamic of immiscible polymers and interface width of miscible system have been achieved, the interdiffusion kinetics at a level of polymer chain size is still absent now.

EXPERIMENTAL

Materials

Poly(*n*-butyl methacrylate) (P*n*BMA, M_n = 93.9 kDa, PDI = 2.14, Aldrich) and poly(vinyl chloride) (PVC, M_n = 34.7 kDa, PDI = 1.81, Aldrich) were commercial products. Tetrahydrofuran (THF) and SS-218 methyl tin mercaptide were used as received after purchased from Sinopharm Group Chemical Reagent Co., Ltd. (Shanghai, China) and Hubei Nanxing Chemical Co., Ltd. (Hubei, China), respectively.

Sample Preparation

Sample preparation for DSC and miscibility measurements

1 g of the mixtures of P*n*BMA and PVC in 20 mL of THF solution with different weight ratios of PVC/P*n*BMA was cast into films with a thickness of *ca.* 1 mm for DSC measurements. In order to reduce the degradation of PVC at high temperatures during the miscibility measurements, two drops of SS-218 methyl tin mercaptide were added into the THF solution.

Sample preparation for AFM measurements

PVC in THF solution was cast in a culture dish. Then, the solvent evaporated slowly. The film with a thickness of *ca.* 1 mm was kept under vacuum at 30 °C overnight. The P*n*BMA film was compression-molded under 20 MPa at 80 °C for 30 min. Before laminating, PVC and P*n*BMA sheets were pretreated to make the surface smooth. First, silicon wafers were ultrasonically cleaned in acetone for 5 min, rinsed with deionized water, dried with compressed nitrogen. P*n*BMA and PVC sheets were put between two clean silicon wafers with weights above and heated for 2 h at 80 °C and 110 °C, respectively. Secondly, P*n*BMA and PVC were laminated at 110 °C or 75 °C for different time. The smooth plane across the interdiffusion interface of the laminate was obtained from ultramicrotomy with a diamond knife on a UCT-GA-D/E-1/00 machine (Leica, Austria).

Instruments and Measurements

LCD parameters tester

Measurements of the transmission as a function of temperature were performed on an LCD parameters tester (LCT-5016C, Changchun Liancheng Instrument Co. Ltd.). A halogen lamp was used as an incident light source. The onset point was used to determine the cloud point of the mixed blend.

Differential scanning calorimetry (DSC)

The DSC measurements were carried out on a DSC-Q2000 (TA Inc., USA) at a heating rate of 20 K/min. The glass transition behavior was investigated in temperature range from −20 °C to 120 °C. Inflection point method was used to determine the glass transition temperature T_g of the blend.

Atomic force microscopy

AFM analysis was performed on a scanning probe microscope (SPA-400, Seiko Instruments Inc., Japan). A silicon probe (Mikro Masch Inc., Estonia) with a typical cantilever length of 230 μm was used. The nominal spring constant and resonance frequencies of the probe were 25–60 N/m and 150–190 kHz, respectively. The tip radius of curvature was *ca*. 10 nm. The topography and phase images were detected in tapping mode at room temperature. The information of interface was obtained from phase images.

RESULTS AND DISCUSSION

Phase Diagram of PVC/PnBMA Blends

Figure 1 shows the temperature dependence of normalized transmittance of PVC/P*n*BMA blends with 50 wt%–95 wt% of PVC mass. Due to the heavy degradation of polymers in spite of the existence of stabilizer of SS-218 methyl tin mercaptide, the transmittance could not be obtained for the samples with a PVC mass below 50 wt% or above 95 wt%. The onset temperatures, referred as the cloud point, can be calculated. Consequently, the phase diagram is shown in the inset of Fig. 1. This blend exhibited a lower critical solution temperature (LCST) behavior with a critical composition of 90 wt% PVC and a critical temperature of 192 °C, respectively.

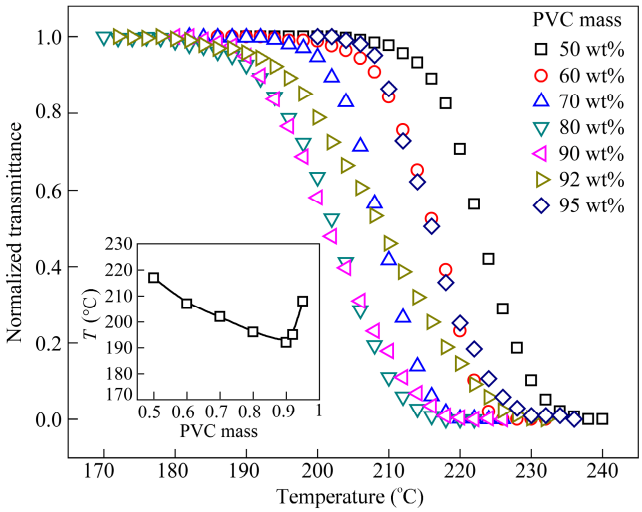


Fig. 1 Temperature dependence of normalized transmittance of PVC/P*n*BMA blends with different PVC contents (Inset is the phase diagram of the blends.)

Miscibility of PVC/PnBMA Blends

The miscibility of P*n*BMA blends can be determined by DSC measurements usually. Each blend showed only a single transition in the DSC curves from −20 °C to 120 °C, indicating that PVC and P*n*BMA were miscible in this temperature range. Their inflection points of the heat flow, *i.e.*, the peak of their derivatives (inset of Fig. 2),

were considered as their glass transition temperatures (T_gs) which increased with the increasing of PVC content. These T_gs could be described by traditional Fried equation, Fox equation and Gordon-Taylor equation well. Without the fitting parameter k, Fox equation was better than Fried equation; but with the parameter $k = 0.99 \pm 0.10$, Gordon-Taylor equation was the best suitable one, where T_gs almost presented a linear relation with PVC content. This was in good agreement with Dlubek's result where Gordon-Taylor relation with $k = 1.5$ worked up to PVC content less than 50 wt%[42].

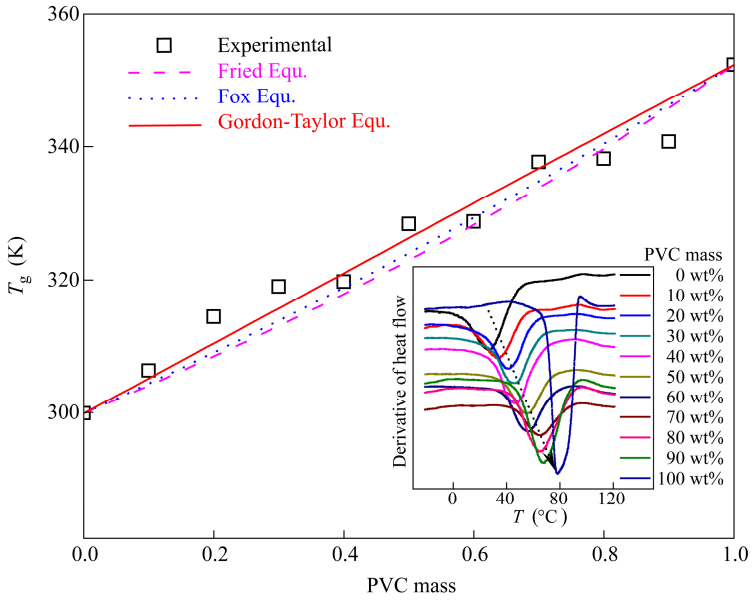


Fig. 2 Glass transition temperature of the blend as a function of PVC content and the fitting lines from Fried (dash line), Fox (dot line) and Gordon-Taylor (solid line) equations
Inset: the temperature dependence of derivative of heat flow obtained from DSC measurements; arrow directs the increasing of PVC content.

Interdiffusion of PVC/PnBMA Laminates

Rubbery/rubbery diffusion behavior

Figure 3 shows the topography and phase images across the interface of PVC/P*n*BMA laminates annealed at 110 °C for different time. The microtoming surfaces are smooth enough to eliminate the topography effect on the analysis of phase images. As a result, in the phase images, the bright and dark regions are ascribed to the stiff PVC and viscoelastic P*n*BMA, respectively[35]. The interface widths (Ls), which can be achieved from the fitting of relative concentration profile across the interface by a hyperbolic tangent function[34], are 30.0, 55.2 and 110.7 nm for 1, 2 and 4 h, respectively. Obviously, L is proportional to the square root of time as shown in Fig. 4, indicating that the interdiffusion obeys Case-I behavior where both PVC and P*n*BMA are rubbery at this annealed temperature. According to the relationship between L and annealing time t, $L = (4D_m t)^{1/2}$, the mutual diffusion coefficient D_m is 2.04×10^{-19} m^2/s, which is consistent with 2.5×10^{-17}–3.5×10^{-17} m^2/s by PALS[23] and 2.0×10^{-18} m^2/s by DSC[42]. Kramer and coworkers proposed that D_m was inversely proportional to the molecular weight (M_n)[13]. For binary system, $D \propto M_{n,1}^{-1} \cdot M_{n,2}^{-1}$. In PALS and DSC methods, the molecular weights of PVC and P*n*BMA were 32 kDa and 103 kDa, respectively, which were similar to those in this work. This result implies that AFM is a reliable and powerful tool to investigate the interdiffusion of polymers.

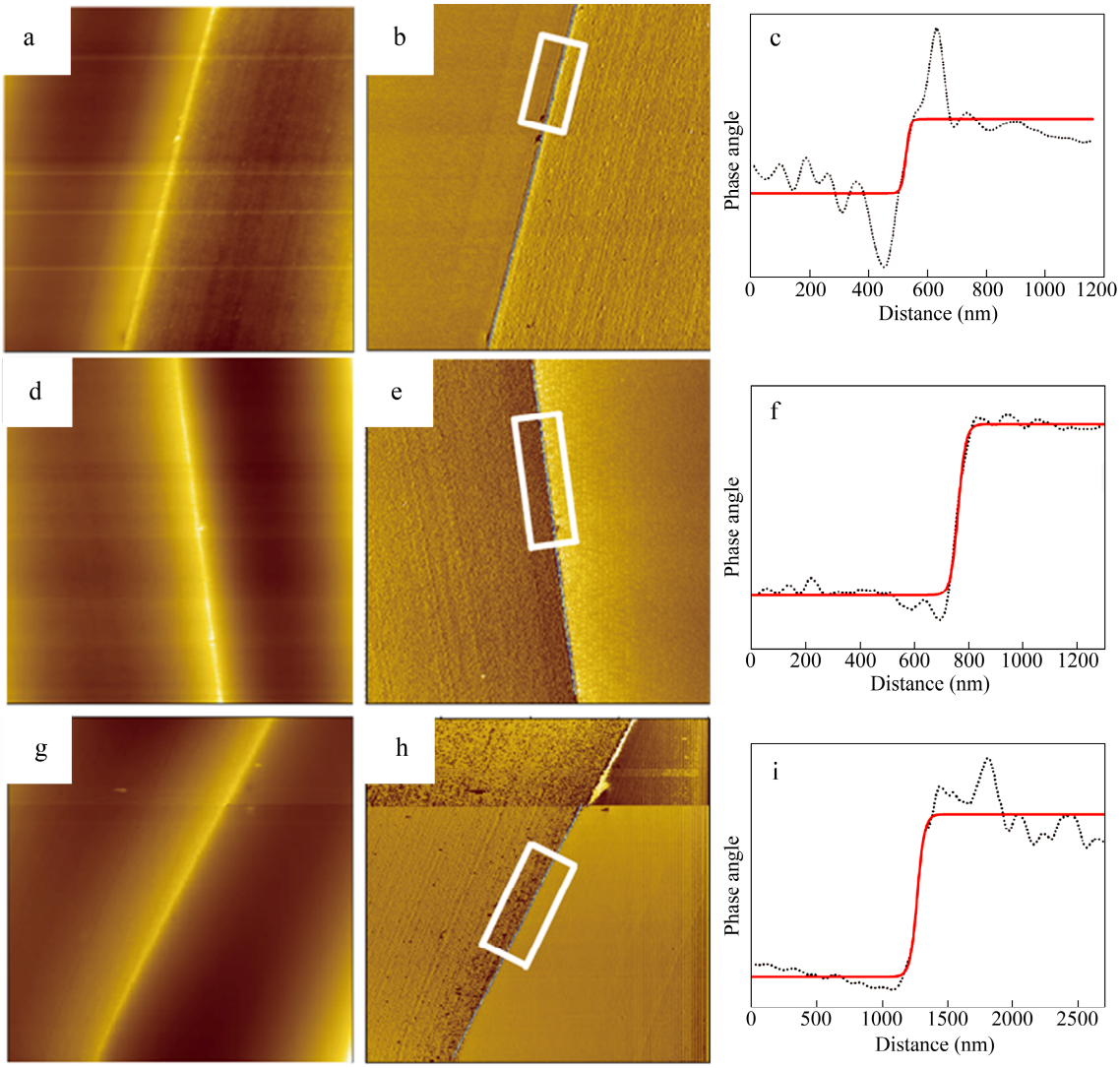


Fig. 3 Topography (a, d, g), phase (b, e, h) images and the corresponding phase degree profiles (c, f, i) highlighted by rectangles across the interfaces of PVC/P*n*BMA laminates annealed at 110 °C for 0.5 h (a–c), 1 h (d–f) and 4 h (g–i) The scanning areas were 10.0 μm × 10.0 μm (a, b, d, e) and 20.0 μm × 20.0 μm (g and h), respectively. *Z* ranges are 211.2 nm (a), 268.4 nm (d), 549.0 nm (g), and 35.9° (b), 19.0° (e), 55.5° (h).

Glassy/rubbery diffusion behavior

Figure 5 shows the topography and phase images across the interface of PVC/P*n*BMA laminates annealed at 75 °C for different time. It is expected that the diffusion would be a glassy/rubbery diffusion because the annealing temperature is between T_gs of PVC and P*n*BMA. The *L*s are 26.3, 58.1 and 150.7 nm for 16, 37 and 96 h, respectively. As expected, the diffusion obeys Case-II behavior because *L* is proportional to the annealing time (Fig. 6). This glassy/rubbery diffusion is similar to the swelling and dissolution process of polymer by solvents or small molecules. The glassy PVC is plasticized and swollen by the rubbery P*n*BMA. Once the plasticized region is large enough, PVC can be disentangled and dissolved[43]. The penetration velocity, *i.e.*, the slope of the fitting line, is 4.36×10^{-13} m/s. This value is consistent with that obtained from the thin bilayers of rubbery polystyrene on glassy poly(2,6-dimethyl-1,4-phenylene oxide) investigated by SIMS (0.2×10^{-10}–1.1×10^{-10} m/s for PS with different molecular weight at 180 °C)[27] and of rubbery poly(vinyl methyl ether) on glassy polystyrene at 76 °C observed by specular neutron reflection and spectroscopic ellipsometry (*ca.* 6×10^{-11} m/s)[44].

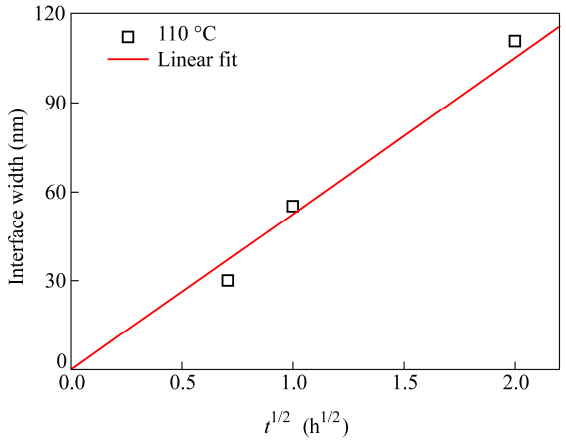


Fig. 4 Interface width for PVC/P*n*BMA laminates annealed at 110 °C as a function of the square root of annealing time

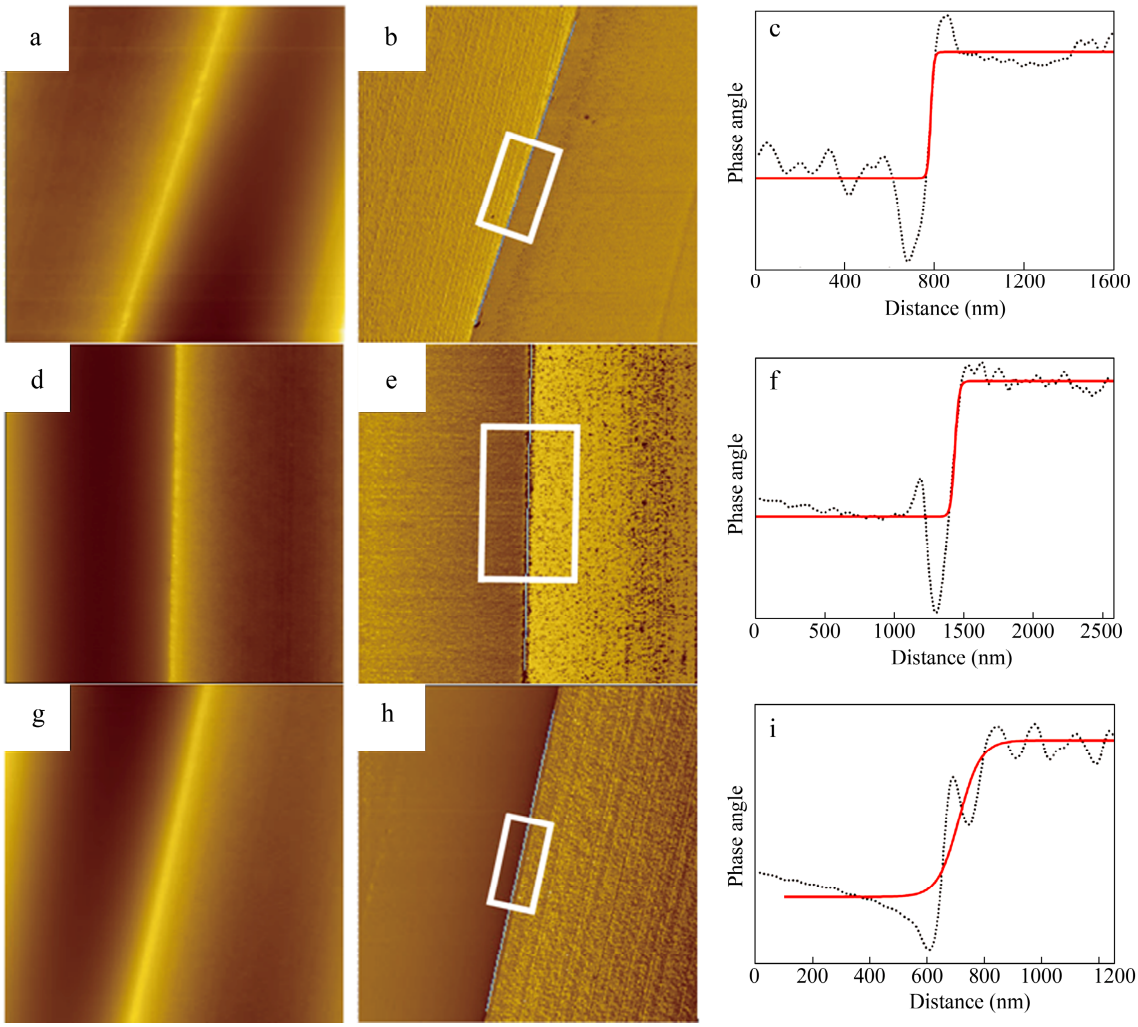


Fig. 5 Topography (a, d, g), phase (b, e, h) images and the corresponding phase degree profiles (c, f, i) highlighted by rectangles across the interfaces of PVC/P*n*BMA laminates annealed at 75 °C for 16 h (a–c), 37 h (d–f) and 96 h (g–i) The scanning areas were 10.0 μm × 10.0 μm for all AFM images. *Z* ranges are 419.0 nm (a), 139.3 nm (d), 588.1 nm (g), and 24.8° (b), 53.7° (e), 24.5° (h).

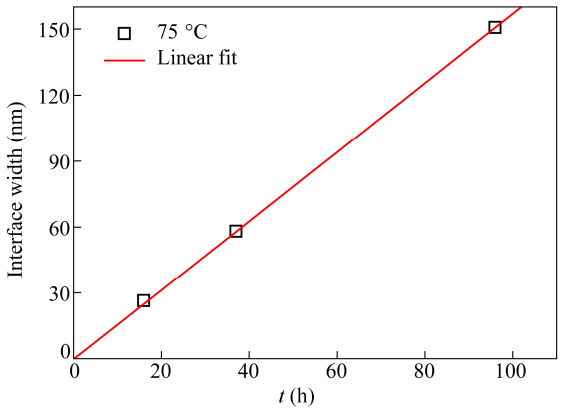


Fig. 6 Annealing time dependence of the interface width for PVC/P*n*BMA laminates annealed at 75 °C

Comparison between rubbery/rubbery and glassy/rubbery diffusion behaviors

To identify the Case-II and Case-I diffusion behaviors at a nanoscale, the scanning area was set as 1.0 μm × 1.0 μm. Many loose P*n*BMA chains aggregate at the glassy/rubbery interface because P*n*BMA diffuses faster than PVC at 75 °C (Fig. 7b). However, this phenomenon disappears for rubbery/rubbery interdiffusion in Fig. 7(d). Figure 7(e) exhibits the grain size of 30 nm. Considering the tip amplification effect from the commercial tip radius of 10 nm, the real grain size is *ca*. 20 nm. The unperturbed root mean square radius of gyration of P*n*BMA, $R_g = (Nb^2/6)^{1/2}$, is 7.35 nm, where N and b are degree of polymerization and statistic segment length (*ca*. 0.7 nm), respectively. Namely, there are 2—3 P*n*BMA chains in each grain. In a word, the interdiffusion at a level of polymer chain size can be observed in real space by this technique.

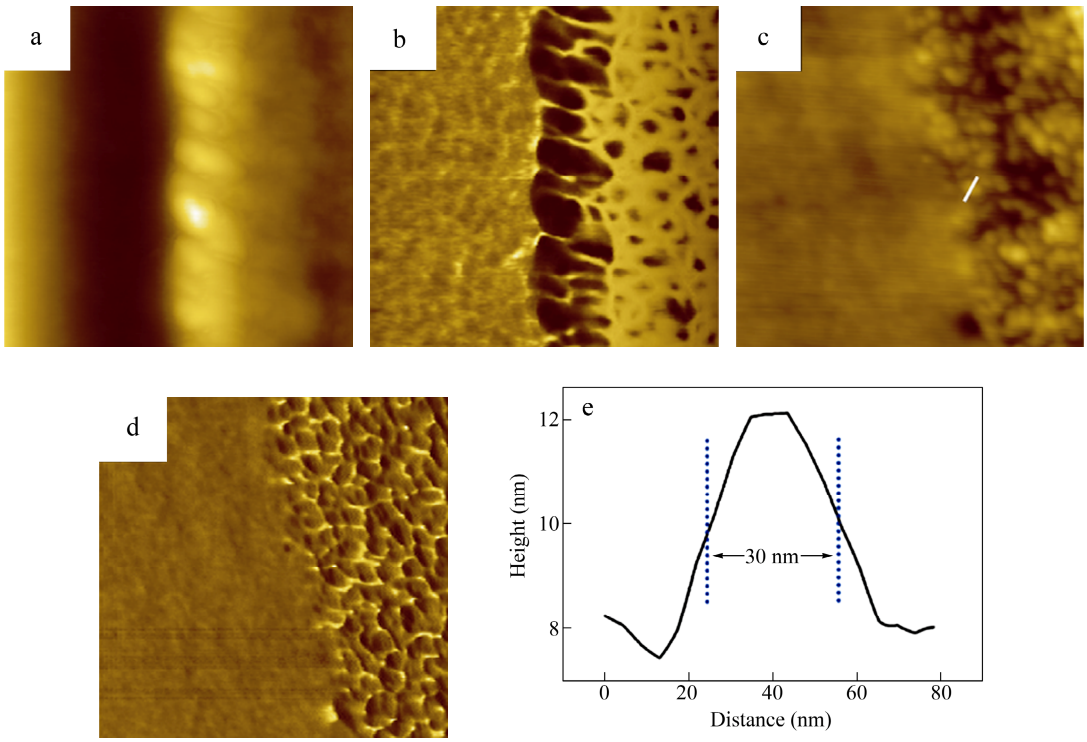


Fig. 7 Topography (a, c) and corresponding phase (b, d) images across the interface of PVC/P*n*BMA laminates annealed at 75 °C for 37 h (a, b) and at 110 °C for 4 h (c, d)
The scanning areas were 1.0 μm × 1.0 μm for all AFM images. *Z* ranges are 33.2 nm (a), 18.8 nm (c), and 62.4° (b), 61.8° (d). (e) is the cross-section profile of the highlighted line in (c).

CONCLUSIONS

In this work, the miscibility of PVC/P*n*BMA blends and the interdiffusion of PVC/P*n*BMA laminates have been investigated by DSC and AFM, respectively. This blend exhibited a lower critical solution temperature (LCST) behavior with a critical composition of *ca*. 90 wt% PVC and a critical temperature of 192 °C. Combined with topography and phase images of TM-AFM, the relative concentration profile, interface width and the relationship between interface width and annealing time were achieved. At 110 °C, the diffusion obeyed a typical Fickian Case-I diffusion behavior where the interface width was proportional to the square root of annealing time. The mutual diffusion coefficient was in good agreement with that obtained from DSC and PALS, respectively. However, at 75 °C, the diffusion followed a typical Case-II diffusion behavior where the interface width was proportional to annealing time. These results imply that AFM is a reliable and powerful tool for the investigation of polymer/polymer interdiffusion at a level of polymer chain size.

ACKNOWLEDGEMENTS We thank the HUST Analytical and Testing Center for allowing us to use its facilities.

REFERENCES

1 Jeon, J.H., Monne, H.M.S., Javanainen, M. and Metzler, R., Phys. Rev. Lett., 2012, 109: 188103
2 Dilanji, G.E., Langebrake, J.B., De Leenheer, P. and Hagen, S.J., J. Am. Chem. Soc., 2012, 134: 5618
3 Xiao, L.H., Wei, L., Liu, C., He, Y. and Yeung, E.S., Angew. Chem.-Int. Ed., 2012, 51: 4181
4 Cho, H.W., Kwon, G., Sung, B.J. and Yethiraj, A., Phys. Rev. Lett., 2012, 109: 155901
5 Lehmann, S., Seiffert, S. and Richtering, W., J. Am. Chem. Soc., 2012, 134: 15963
6 Flier, B.M.I., Baier, M.C., Huber, J., Mullen, K., Mecking, S., Zumbusch, A. and Woll, D., J. Am. Chem. Soc., 2012, 134: 480
7 Pang, H., Zhong, G.J., Xu, J.Z., Yan, D.X., Ji, X., Li, Z.M. and Chen, C., Chinese J. Polym. Sci., 2012, 30(6): 879
8 Farago, J., Meyer, H. and Semenov, A.N., Phys. Rev. Lett., 2011, 107: 178301
9 Xu, L., Zhong, G.J., Ji, X. and Li, Z.M., Chinese J. Polym. Sci., 2011, 29(5): 540
10 Edwards, S., Proc. Phys. Soc., 1967, 92: 9
11 de Gennes, P.G., J. Chem. Phys., 1971, 55: 572
12 Brochard, F., Jouffroy, J. and Levinson, P., Macromolecules, 1983, 16: 1638
13 Kramer, E.J., Green, P. and Palmstrøm, C.J., Polymer, 1984, 25: 473
14 Brochard, F. and De Gennes, P., Europhys. Lett., 1986, 1: 221
15 Kunz, K. and Stamm, M., Macromolecules, 1996, 29: 2548
16 Composto, R. and Kramer, E., J. Mater. Sci., 1991, 26: 2815
17 Composto, R.J., Kramer, E.J. and White, D.M., Macromolecules, 1992, 25: 4167
18 Sferrazza, M., Xiao, C., Jones, R.A.L., Bucknall, D.G., Webster, J. and Penfold, J., Phys. Rev. Lett., 1997, 78: 3693
19 Klein, J., Science, 1990, 250: 640
20 Shearmur, T., Clough, A., Drew, D., Van Der Grinten, M. and Jones, R., Phys. Rev. E, 1997, 55: 3840
21 Clarke, N., Colley, F.R., Collins, S.A., Hutchings, L.R. and Thompson, R.L., Macromolecules, 2006, 39: 1290
22 Harton, S.E., Koga, T., Stevie, F.A., Araki, T. and Ade, H., Macromolecules, 2005, 38: 10511
23 Dlubek, G., Pionteck, J., Bondarenko, V., Pompe, G., Taesler, C., Petters, K. and Krause-Rehberg, R., Macromolecules, 2002, 35: 6313
24 Price, K.E., Broadwater, S.J., Bogdan, A.R., Keresztes, I., Steinbacher, J.L. and McQuade, D.T., Macromolecules, 2006, 39: 7681
25 Jabbari, E. and Peppas, N.A., Macromolecules, 1993, 26: 2175
26 Tomba, J.P., Carella, J.M., García, D. and Pastor, J.M., Macromolecules, 2004, 37: 4940
27 Lin, H., Tsai, I., Yang, A.C.M., Hsu, M. and Ling, Y., Macromolecules, 2003, 36: 2464

28 Zheng, X., Rafailovich, M., Sokolov, J., Strzhemechny, Y., Schwarz, S., Sauer, B. and Rubinstein, M., Phys. Rev. Lett., 1997, 79: 241
29 Kressler, J., Higashida, N., Inoue, T., Heckmann, W. and Seitz, F., Macromolecules, 1993, 26: 2090
30 Siangchaew, K. and Libera, M., Macromolecules, 1999, 32: 3051
31 Gao, S.L. and Mäder, E., Compos. Pt. A-Appl. Sci. Manuf., 2002, 33: 559
32 Paradkar, R.P., Li, J., Bar, G., Pham, H., Bosnyak, C. and Weinhold, J., J. Appl. Polym. Sci., 2007, 106: 1507
33 Bresson, B., Portigliatti, M., Salvant, B. and Fretigny, C., J. Appl. Polym. Sci., 2008, 109: 602
34 Liao, Y.G., Nakagawa, A., Horiuchi, S. and Ougizawa, T., Macromolecules, 2007, 40: 7966
35 Liao, Y.G., Su, Z.H., Ye, X.G., Li, Y.Q., You, J.C., Shi, T.F. and An, L.J., Macromolecules, 2005, 38: 211
36 You, J.C., Liao, Y.G., Men, Y.F., Shi, T.F., An, L.J. and Li, X.L., Macromolecules, 2011, 44: 5318
37 You, J.C., Liao, Y.G., Men, Y.F., Shi, T.F. and An, L.J., Langmuir, 2010, 26: 14530
38 You, J.C., Hu, S.S., Liao, Y.G., Song, K.X., Men, Y.F., Shi, T.F. and An, L.J., Polymer, 2009, 50: 4745
39 You, J.C., Shi, T.F., Liao, Y.G., Li, X.L., Su, Z.H. and An, L.J., Polymer, 2008, 49: 4456
40 Liao, Y.G., You, J.C., Shi, T.F., An, L.J. and Dutta, P.K., Langmuir, 2007, 23: 11107
41 Liao, Y.G., Su, Z.H., Sun, Z.Y., Shi, T.F. and An, L.J., Macromol. Rapid Commun., 2006, 27: 351
42 Dlubek, G., Pompe, G., Pionteck, J., Janke, A. and Kilburn, D., Macromol. Chem. Phys., 2003, 204: 1234
43 Nguyen, V.N., Perrin, F.X. and Vernet, J.L., Corros. Sci., 2005, 47: 397
44 Sauer, B.B. and Walsh, D.J., Macromolecules, 1991, 24: 5948